Suppression of Fragmentation in Mass Spectrometry

Siddihalu, Lakshitha Madunil
Faculty of Design, Kyushu University

Imasaka, Totaro
Division of International Strategy, Center of Future Chemistry, Kyushu University

Imasaka, Tomoko
Faculty of Design, Kyushu University

出版情報：Analytical chemistry. 92 (24), pp.16016-16023, 2020-12-02. American Chemical Society
バージョン：
権利関係：

Suppression of Fragmentation in Mass Spectrometry

S. Lakshitha Madunil,[♯] Totaro Imasaka[†,‡] and Tomoko Imasaka[♯*]

[♯]*Faculty of Design, Kyushu University, 4-9-1, Shiobaru, Minami-ku, Fukuoka 815-8540: 744 Motooka, Nishi-ku, Fukuoka 819-0395, Japan*

[†]*Division of International Strategy, Center of Future Chemistry, Kyushu University,744 Motooka, Nishi-ku, Fukuoka 819-0395, Japan*

[‡]*Hikari Giken, Co., 2-10-30, Sakurazaka, Chuou-ku, Fukuoka 810-0024, Japan*

* To whom correspondence should be addressed. E-mail: imasaka@design.kyushu-u.ac.jp

ABSTRACT: Suppressing fragmentation is a constant challenge in mass spectrometry, since a molecular ion can readily be identified and provides information concerning the molecular weight of an analyte. Several techniques such as charge exchange chemical ionization (CECI) and vacuum ultraviolet emission ionization (VUVEI) have been developed to date for achieving this purpose. In this study, we report on the use of tunable ultraviolet (UV) and near-infrared (NIR) femtosecond (fs) lasers (35 fs) for the multiphoton ionization (MPI) of *cis*- and *trans*-4-methylcyclohexanols, the reference molecules that are currently used to examine fragmentation suppression. The results obtained here were compared with those obtained by CECI and VUVEI, since they were reported as the best techniques for suppressing fragmentation. A molecular ion was strongly enhanced by carefully minimizing the excess energy in the ionic state using tunable UV and NIR fs-lasers. The ratio of the intensities for molecular and fragment ions, $[M]^+/[M-H_2O]^+$, increased significantly (9.5 fold and 8.5 fold for *cis*- and *trans*-isomers, respectively, in UV fs-MPI) compared to the values obtained by CECI and VUVEI, respectively.

Mass spectrometry (MS) is an indispensable tool for the analysis of organic compounds not only in the basic sciences such as physics/chemistry/biology but also in numerous applications such as environmental/forensic sciences.[1-3] High-resolution MS based on Fourier transform ion cyclotron resonance or time-of-flight is useful for accurate mass-to-charge ratios (*m/z*) to be measured and then for determining the chemical formula of the analyte.[4-6] However, when a molecular ion is not significant and is difficult to be identified, even molecular weight cannot be determined.

Electron ionization (EI) is the most commonly used technique in MS. In general, organic compounds have ionization energies (*IEs*) in the range from 7 to 15 eV.[7] In EI, an electron is typically accelerated to 70 eV to increase the ionization efficiency, which leads to extensive fragmentation in many cases. For example, a molecular ion is missing or is very weak for alcohols, because they easily undergo dehydration and fragmentation. For this reason, EI, which is commonly used in MS, is not suitable for the analysis of alcohols in a complex sample mixture, since a very similar fragment pattern can occasionally be observed even for the alcohols with different molecular weights. Accordingly, suppression of fragmentation is crucial in MS to identify the molecule and to improve the selectivity in its analysis.

Many techniques have been developed to date to achieve soft ionization in attempts to observe a molecular ion. Chemical ionization (CI), electron capture ionization, field ionization (FI), field desorption ionization (FDI), and fast atom bombardment ionization are all well-known traditional techniques but all have certain limitations. For example, numerous adduct ions are observed in CI, making the identification of a molecular ion difficult. Electro spray ionization (ESI) and matrix-assisted laser desorption ionization (MALDI) have been developed more recently and have been successfully applied especially for macromolecules.[8] However, there are also several drawbacks to these techniques. For example, multiply-charged ions are formed in ESI (as well as in FI and FDI), and combining MALDI with a separation technique is difficult in terms of measuring a sample mixture in a complex matrix.

Substituted cyclohexanols are currently used to evaluate ionization techniques in MS. In fact, *cis*- and *trans*-4-methylcyclohexanols, the chemical structures of which are shown in Figure 1, are typically employed to compare fragmentation suppression (see a textbook of "Mass Spectrometry" written by J. H. Gross), since a hydration reaction easily occurs especially for *trans*-isomer.[9] A technique referred to as charge exchange chemical ionization (CECI) or charge transfer chemical ionization has been successfully used for fragmentation suppression, since the excess energy involved in the dissociation of a molecular ion can be reduced by choosing a reagent gas with a recombination energy that is nearly equal to the ionization energy (*IE*) of the analyte molecule. Note that these stereoisomers are also studied by survivor-ion spectrometry producing ions by electron ionization and

submitting them without mass selection to collisional neutralization and reionization followed by selective monitoring of non-dissociating ions.[10]

Photoionization has also been employed for soft ionization, since the excess energy can be controlled by changing the wavelength of the light source.[11,12] Vacuum ultraviolet emission ionization (VUVEI) is useful for single-photon ionization to suppress fragmentation.[13-15] A pulsed laser has been utilized for multiphoton ionization (MPI).[16-18] A nanosecond laser with a narrow band width has a distinct advantage for selective ionization by using the first photon for excitation and the subsequent photon for ionization, a process that is referred to as resonance-enhanced two-photon ionization (RE2PI) or more generally as resonance-enhanced multiphoton ionization (REMPI). This technique is especially useful when a molecule is cooled by supersonic jet expansion, because of a narrow spectral band width in the absorption spectrum. However, this technique is only valid for a molecule with an electronic excited state at an energy lower than half of the *IE*, e.g., aromatic compounds such as benzene. However, it is not suitable for a molecule with a short-excited state lifetime by efficient relaxation to triplet levels by intersystem crossing or to a ground state by internal conversion.[19] Then, observing a molecular ion becomes difficult when many heavy atoms such as chlorines/bromines or nitro groups are present in a molecule.

A molecule can be ionized without using an intermediate state, a process that is referred to as nonresonant two-photon ionization (NR2PI) or more generally as nonresonant multiphoton ionization (NRMPI). This process is essential for a molecule, in which the energy of an electronic excited state is higher than half of the *IE*, e.g., aliphatic compounds such as cyclohexane. In this case, the excess energy can be reduced to zero by adjusting the laser wavelength to half the value of the *IE*. However, the efficiency of NR2PI is lower than that of RE2PI in the case of nanosecond ionization. It is possible to increase the ionization efficiency by increasing the laser pulse energy and by focusing the laser beam tightly. This approach, however, suffers from dominant fragmentation. It has been reported that the efficiency of NR2PI can reach the level of RE2PI when the pulse width of the laser is reduced to ca. 50 fs.[20,21] Therefore, this approach, which is referred to as femtosecond (fs) ionization, has been utilized to observe a molecular ion for various compounds, e.g., non-aromatic highly-flexible molecules such as triacetone triperoxide and toxic/carcinogenic molecules such as pesticides that contain numerous heavy atoms and nitro groups.[21,22] Another approach is FI using an intense NIR femtosecond laser. Photodissociation dynamics has been studied for acetophenone by a pump-probe technique using transform-limited/chirp pulses.[23] The ionization efficiency is reported to depend on the positive/negative chirp of the pulse for structural isomers.[24,25] However, no systematic research has been conducted to compare the ability of fragmentation suppression with other established techniques such as CECI and VUVEI.

In this study, we examined the best technique for observing a molecular ion using *cis*-and *trans*-4-methylcyclohexanols as reference molecules, in which tunable ultraviolet (UV) and near-infrared (NIR) fs-lasers were used for NR2PI and NRMPI, respectively, and compared the results with data obtained using CECI and VUVEI. As a result, NR2PI using a tunable UV fs-laser was found to be the best (a tunable NIR fs-laser was the second best) for observing a molecular ion. To our knowledge, this is the first report of a systematic study for suppressing fragmentation using the above well-known reference molecules for comparison.

EXPERIMENTAL SECTION

EI-MS. A 1-μL aliquot of a sample containing a mixture of *cis*- and *trans*-4-methylcyclohexanols (0.125 μg/μL for each) was measured using a gas chromatograph (GC) combined with a quadrupole EI-MS (GCMS-QP2010, Shimadzu, Kyoto, Japan). These stereoisomers were obtained from Tokyo Chemical Industry and were used as different chemicals because of a large enthalpy change for transition ($\Delta H_t = 1.7 \pm 0.5$ kJ·mol^{-1}).[26] The temperature of the sample injection port was set at 250 °C and was used as the splitless mode. The flow rate of helium was adjusted at 1 mL/min. The analyte was separated by a DB-5ms column (length 30 m, inner diameter 0.25 mm, film thickness 0.25 μm). The temperature program of the GC oven was as follows; the initial temperature of the capillary column was 50 ºC and was held for 1 min, a ramp of 25 ºC/min to 125 ºC, then the temperature was increased to 200 ºC at a rate of 8 ºC/min and was finally held for 10 min. The electron energy was set at 70 eV. The temperatures of the ion source and the interface between the GC and MS were kept at 230 °C and 280 °C, respectively.

LI-TOF/MS. The analytes in the sample mixture were separated by GC (6890 N, Agilent Technologies, Santa Clara, CA) using a DB-5ms column (length 30 m, inner diameter 0.25 mm, film thickness 0.25 μm). The temperature of the sample injection port was set at 250 ºC. The temperature program of the GC oven was the same as that used in EI-MS. The eluted analytes were measured by a time-of-flight (TOF) MS developed in our laboratory. The molecules were ionized using a tunable femtosecond optical pulse generated by an optical parametric amplifier (OPA, TOPAS, Spectra-Physics, Santa Clara, CA, USA) pumped by a Ti:sapphire laser (TS, 800 nm, 35 fs, 1 kHz, 6 mJ, Solstice Ace, Spectra-Physics). In fact, an UV fs-pulse was generated at 241, 245, 252, 257, and 262 nm using the UV option of the OPA, in addition to the third harmonic emission (267 nm) of the TS (800 nm). The signal beam of the OPA was directly used as an NIR fs-pulse at 1200, 1220, 1240, 1260,

1280, 1300, and 1320 nm. The generated ion was accelerated toward a TOF tube and was detected by a microchannel plate detector (F4655-11, Hamamatsu Photonics, Shizuoka, Japan). The temperature of the interface between the GC and MS was kept at 230 ºC. The signal was acquired by a digitizer (Acqiris AP240, Agilent Technologies) and was processed using a software program developed in our laboratory.

Quantum Chemical Calculation. The spectral properties of the neutral and ionic species of *cis*- and *trans*-4-methyl cyclohexanols were calculated based on density functional theory (DFT). To obtain the minimum geometries, the B3LYP method with a cc-pVDZ basis set was used, and the vertical ionization energy was evaluated from the difference between the energies of the ground and ionic states by wB97XD/cc-pVTZ.[27] The lowest one-hundred singlet transition energies and the oscillator strengths were calculated using time-dependent DFT (TD-DFT) at the level of B3LYP/cc-pVTZ. The UV-visible absorption spectrum was predicted for neutral and ionic species using the GaussView 5 software program. The absorption spectrum of the fundamental and overtone vibrational bands in the infrared (IR) region was calculated by assuming an anharmonic potential and was predicted using the GaussView 5 software program. Cartesian coordinates of the atoms in the *cis*- and *trans*-isomers are listed in Tables S1 and S2, respectively, in the Supporting Information.

RESULTS AND DISCUSSION

Electron Ionization Mass Spectrum. Figure 2 shows the mass spectra for *cis*- and *trans*-4-methylcyclohexanols measured by EI. The molecular ion was very small for the *cis*-isomer and was not detected for the *trans*-isomer. The observed fragment patterns were very similar, thus making it difficult to differentiate the isomers using library reference data. The results were nearly identical to those measured based on EI, although the fragment pattern of *cis*-4-methylcyclohexanol is slightly different from that of *trans*-4-methylcyclohexanol in survivor-ion mass spectrometry.[10] From the *m/z* value, the signal peaks can be assigned to the molecular ion at m/z = 114 and the fragment ions of $C_7H_{12}^+$, $C_6H_9^+$, $C_5H_{10}^+$, $C_3H_5O^+$ at m/z = 96, 81, 70, 57, respectively. EI is based on the inelastic scattering of electrons, and a portion of the energy in an electron accelerated typically to 70 eV is transferred to a molecule for ionization and subsequent dissociation, the efficiency of which depends on the incident angle of the electron in the collision. Therefore, it is difficult to control the excess energy remaining in the ionic state.

Ionization Mechanism. There are two types of major schemes in fs-ionization, i.e., FI and MPI. A strong electric field induced by a femtosecond optical pulse is applied to an electron in a molecule and the electron is eventually ejected by a ponderomotive force to generate an ion, which is referred

to as FI or tunneling ionization. A Keldysh parameter ($\gamma = (I_p/2U_p)^{1/2} = (E_i/1.87\times10^{-13}I\lambda^2)^{1/2}$ can be used to differentiate the FI and MPI mechanisms, in which I_p is the potential energy, U_p is the ponderomotive energy, E_i is the zero-field ionization potential expressed in eV, I is the laser intensity in W/cm^2, λ is the laser wavelength in a unit of μm, and the kinetic energy can be calculated by $K = 3.17 \times U_p$.[28,29] FI is dominant at γ <1, which is in contrast to MPI at γ >1. Note that FI is important when a higher-peak-power laser emitting at longer wavelengths is used for ionization.

The Keldysh parameters calculated under the experimental conditions are summarized in Table S3 in the Supporting Information. The values for the UV ionization were 4.19 - 4.22 because of a short wavelength (241 - 267 nm) and a small pulse energy (25 μJ). On the other hand, the values were 1.32 - 1.34 for NIR ionization. Note that the kinetic energy of an electron is in the range of 8.40 - 8.43 eV and would be inefficient for the re-scattering of an electron in a molecule by the electron ejected by the Ponderomotive force. A molecule is therefore mainly ionized by MPI in this study, although the FI process cannot be completely ruled out in NIR ionization. As shown in Figure 3(A), a molecule can be ionized either by two or three photons in UV ionization, which is in contrast to the ten or eleven photons required in NIR ionization. The absorption spectra calculated for the neutral molecule derived from *cis*- and *trans*-4-methylcyclohexanols are shown in Figure S1 in the Supporting Information. Since no absorption band is located in the UV region, the molecule can be ionized by NR2PI or nonresonant three-photon ionization (NR3PI). The excess energy remaining in the molecular ion is small in 2PI but is very large in 3PI. As shown in Figure S2 in the Supporting Information, a molecular ion has no absorption band in the NIR region (1220-1320 nm) and, as a result, fragmentation by absorbing additional NIR photons would be negligible.

In the model shown in Figure 3(B), in theory, the signal intensity of the molecular ion increases as a step function above the *IE* (see curve (1)). However, a molecule can be ionized even at lower energies by a transition from vibrational levels in the ground state to Rydberg states by an electric field induced by the optical pulse and by the potential applied by electrodes in MS, which accelerates the ionization by the Stark effect (curve (2)). On the other hand, the signal intensity of the molecular ion decreases by dissociation due to the excess energy in the ionic state (curve (3)). Fragment ions are produced by absorbing additional photons, e.g., a total of three or eleven photons in the UV and NIR regions, respectively, the intensity of which is nearly independent of the photon energy below the *IE* and gradually increases as the molecular ion dissociates with increasing excess energy above this value (curve (4)).

UV Ionization. Figures 4 and 5 show the mass spectra for *cis*- and *trans*-4-methylcylohexanols, respectively, measured at different laser wavelengths in the UV region. A molecular ion was clearly observed in all the data except at 267 nm. Therefore, fs-MPI is superior to EI in terms of observing a

molecular ion. Figures 6 (A) and (B) show the dependences of the laser wavelength on the ratio, $[M]^+/[M\text{-}H_2O]^+$, for the *cis*- and *trans*-4-methylcyclohexanols, respectively (the dependences on the signal intensity, $[M]^+$, are shown in Figure S3 in Supporting Information). The maximal value was observed at 9.84 and 9.63 eV for the *cis*- and *trans*-isomers, respectively. Based on the model shown in Figure 3, these values are considered to be the *IE*s for these compounds. It was difficult to observe a molecular ion exclusively even after optimizing the laser wavelength, suggesting non-adiabatic ionization due to a small (or negligible) Franck Condon factor for a transition between the ground states for neutral and ionic species (see Figure S4 in Supporting Information for more detailed explanation). The observed values are in reasonable agreement with the theoretical values of the vertical ionization (9.77 and 9.65 eV) calculated for *cis*- and *trans*-isomers, respectively (see broken lines in Figures 6 (A) and (B)). These results suggest that the excess energy should be minimal for observing a molecular ion. The half width at half maximum (HWHM) at higher energies was 0.064 and 0.088 eV (520 and 710 cm^{-1}) for the *cis*- and *trans*-isomers, respectively. The spectral line width (a full width at half maximum, FWHM) of the 35-fs pulse was calculated to be 0.052 eV or 420 cm^{-1} (0.026 eV or 210 cm^{-1} for HWHM). These results suggest that 4-methylcyclohexanols are very amenable to undergoing dissociation. This is one of the reasons for why these compounds are frequently used as reference molecules in studies of fragmentation suppression. The value of HWHM at lower energies was 0.100 and 0.079 eV (810 and 640 cm^{-1}) for the *cis*- and *trans*-isomers, respectively. A spectral width arising from the population in the vibrational levels of the ground state can be roughly estimated to be 0.026 eV (210 cm^{-1}) by assuming a thermal energy spread of kT, where k is the Boltzmann constant and T is the absolute temperature. The larger number (0.100-0.079 > 0.026 eV) can be attributed to the ionization via Rydberg states, which was not taken into account in this study. It should be noted that the molecular ion was seldom observed at 267 nm, as shown in Figures 4 (F) and 5 (F), suggesting that only fragment ions were produced by 3PI, which provides a large excess energy that can be used for the dissociation of a molecular ion.

NIR Ionization. Figures 7 and 8 show mass spectra for *cis*- and *trans*-4-methylcylohexanols, respectively, measured at different laser wavelengths in the NIR region. A molecular ion was clearly observed in the NIR region in all cases. It therefore appears that fs-MPI is superior to EI in terms of observing a molecular ion. Figures 9 (A) and (B) show the dependences of the laser wavelength on the ratio, $[M]^+/[M\text{-}H_2O]^+$, for the *cis*- and *trans*-4-methylcyclohexanols, respectively (the dependences on the signal intensity, $[M]^+$, are shown in Figure S5 in Supporting Information). The variation in the signal intensity is relatively small in the NIR compared to that in the UV region, which can be explained by a smaller excess energy in the NIR ionization due to the smaller energy of the NIR photon (see Figure 3 (A)). As shown in Figure 9 (A), the maximum value was obtained at 9.84 eV for the *cis*-

isomer, which coincides with the value obtained in UV ionization (9.84 eV). For the *trans*-isomer, a maximum value was obtained at 9.84 eV as shown in Figure 9 (B), which is nearly equal to or slightly larger than the value observed in UV ionization (9.64 eV). Accordingly, the excess energy should be minimal for observing a molecular ion.

It is interesting to note that the ratio, $[M]^+/[M\text{-}H_2O]^+$, increased at longer wavelengths (smaller photon energies) in both of the data shown in Figures 9 (A) and (B). These signal increases can be attributed to eleven-photon ionization (11PI). In this case, the maximum should appear at a single-photon energy of 9.84/11= 0.895 eV (1386 nm), suggesting that the minimum should appear at (0.984 + 0.895)/2 = 0.940 eV (1318 nm) (see the arrow in Figures 9 (A) and (B)). As mentioned above, the signal at 1318 nm in the observed data was increased. The reason for this discrepancy cannot be explained clearly. However, an overtone absorption band calculated for a C-H stretching vibration by density functional theory is located at around 7036 cm^{-1} (1421 nm) for the *cis*-isomer (7026 cm^{-1} or 1423 nm for the *trans*-isomer), as shown in Figure S6 in the Supporting Information. In this case, MPI would partly be assisted by the vibrational excitation in the NIR, although further investigation will be needed to confirm this.

Photodissociation Pathways. The ratio, $[M]^+/[M\text{-}H_2O]^+$, is consistently larger for the *cis*-isomer than for the *trans*-isomer (cf. Figures 6 (A) vs. (B) and Figures 9 (A) vs. (B)), suggesting that the *trans*-isomer has a more dissociative nature. The peak observed at m/z = 96 can be attributed to the fragment ion $[C_7H_{12}]^+$, which is formed by the elimination of H_2O from the molecular ion. There are several pathways for producing this fragment ion. For example, an H atom bound to C2, C3, C4, C7 can dissociate as H_2O by combining with the OH group at the C1 position (the notation for the carbon atoms is shown in Figure 1). A study using deuterium-labeled isomers reported that the eliminated H_2O is produced by the dissociation of H bound to C2, C3, C4. while the dissociation of H on C7 has not been examined due to unavailability of the deuterated compound with a CD_3 group.[14,15] These findings suggest that the major pathway involves the dissociation of H combined with C4 and C3 to form an additional ring.[30] The distance (2.58 Å) between the O and H bound to C4 in the *trans*-isomer is relatively short (see Figure 1), which would have an accelerating effect on the elimination reaction. However, the distance (2.52 Å) between O and H bound to C7 in the *cis*-isomer is much shorter than this value. As is well known, a primary H is more stable than a tertiary H. In fact, the H-C7 distance (1.10053 Å) in the *cis*-isomer is shorter than the H-C4 distance (1.10374 Å) in the *trans*-isomer, suggesting that the H-C7 bond in the *cis*-isomer is stronger than the H-C4 bond in the *trans*-isomer. Note that the distance (4.41889 Å) between the O and H bound to C4 in the *cis*-isomer is relatively long, and this tertiary H is protected by the CH_3 group combined with C4, resulting in a large potential barrier to dissociation. As a result, the *trans*-isomer would be more likely to undergo

dissociation than the *cis*-isomer, as was found in this study.

Comparison with Other Ionization Techniques. Several techniques have been developed to enhance a molecular ion for 4-methylcyclohexanols and the results are summarized in Table 1. As predicted, EI is not suitable for observing a molecular ion, although it would have been enhanced at lower electron energies (< 70 eV). In CECI, the molecular ion can be enhanced by the choice of a suitable reagent gas. In fact, the use of $C_6F_6^+$ as a reagent gas was found to be optimal especially for the *cis*-isomer.[31] In contrast, a VUV light source is useful especially for the *trans*-isomer. A Lyman-α line source emitting at longer wavelengths (121.6 nm) is more preferential than a He line source (58.4 nm), due to a smaller excess energy in the ionic state.[14,15] Both approaches using UV and fs-NIR lasers are superior to the other best methods reported to date. The values, $[M]^+/[M\text{-}H_2O]^+$, obtained for the *cis*- and *trans*-isomers using CECI and Lyman-α line are also plotted on the data obtained by the UV ionization in Figures 6 (A) and (B), respectively. It is apparent that the values were significantly enhanced (9.5 fold and 8.5 fold for the *cis*- and *trans*-isomers, respectively) by reducing the excess energy by optimizing the wavelength of the UV fs-laser. Similar trends (2.9 fold and 1.8 fold for the *cis*- and *trans*-isomers, respectively) were also observed in the NIR ionization, as shown in Figures 9 (A) and (B). Thus, a technique based on NR2PI using a tunable fs-laser can be quite useful for observing a molecular ion. The ratio of $[M]^+/[M\text{-}H_2O]^+$ measured by VUV ionization was similar to the value measured by fs-ionization at the same excess energy (see Figures 6 and 9), suggesting that a ratio similar to fs-ionization can be obtained using a tunable VUV light from a synchrotron radiation facility.

CONCLUSION

In this study, we employed tunable UV and NIR fs-lasers as ionization sources to observe a molecular ion in MS of *cis*- and *trans*-4-methylcyclohexanols. The intensity of the molecular ion was enhanced when the laser wavelength was carefully optimized within an accuracy of 0.164 eV (1330 cm^{-1}) to minimize the excess energy for the *cis*-isomer (0.167 eV or 1360 cm^{-1} for the *trans*-isomer) because of susceptibility of these compounds to undergo dissociation. The ratio, $[M]^+/[M\text{-}H_2O]^+$, is always smaller for the *trans*-isomer than that for the *cis*-isomer. This can be explained by the fact that the O atom is closer to the tertiary H atom more weakly bound to the C4 atom. The present approach using a tunable UV fs-laser for NR2PI (NIR fs-laser for NRMPI as well) has a potential for use in observing a molecular ion generally for a variety of organic compounds.

AUTHOR INFORMATION

Corresponding Author

*Email: imasaka@design.kyushu-u.ac.jp

ORCID

Tomoko Imasaka: 0000-0002-2131-4995

S. Lakshitha Madunil: 0000-0002-8454-9556

Totaro Imasaka - 0000-0003-4152-3257

Notes

The authors declare no competing financial interest.

ACKNOWLEDGEMENTS

This research was supported by a Grant-in-Aid for Scientific Research from the Japan Society for the Promotion of Science [JSPS KAKENHI Grant Numbers 20H02399] and by the Program of Progress 100 in Kyushu University, The Iwatani Naoji Foundation, and 2020 Collaboration Development Fund for a joint program between National Taiwan Normal University and Kyushu University. Quantum chemical calculations were mainly carried out using the computer facilities at the Research Institute for Information Technology, Kyushu University. The authors wish to thank Prof. Noriyuki Igura for the use of GC/EI-MS in the Faculty of Agriculture, Kyushu University. L. M. wishes to acknowledge the Mitsubishi Corporation International Scholarship for financial support.

REFERENCES

(1) Cho, B.; Cho, H. S.; Kim, J.; Sim, J.; Seol, I.; Baeck, S. K.; In, S.; Shin, D. H.; Kim, E. Simultaneous determination of synthetic cannabinoids and their metabolites in human hair using LC-MS/MS and application to human hair. *Forensic Sci. Int.* **2020**, *306*, 110058.

(2) Matsukami, H.; Takemori, H.; Takasuga, T.; Kuramochi, H.; Kajiwara, N. Liquid chromatography–electrospray ionization-tandem mass spectrometry for the determination of short-chain chlorinated paraffins in mixed plastic wastes. *Chemosphere* **2020**, *244*, 125531.

(3) Gorzizaa, R.; Coxb, J.; Limbergera, R. P.; Mora, L. E. A. Extraction of dried oral fluid spots (DOFS) for the identification of drugs of abuse using liquid chromatography tandem mass spectrometry (LC-MS/MS). *Forensic Chem.* **2020**, *19*, 100254.

(4) Hughey, C. A.; Hendrickson, C. L.; Rodgers, R. P.; Marshall, A. G. Elemental composition analysis of processed and unprocessed diesel fuel by electrospray ionization Fourier transform ion cyclotron resonance mass spectrometry. *Energy and Fuels* **2001**, *15*, 1186–1193.

(5) Hughey, C. A.; Hendrickson, C. L.; Rodgers, R. P.; Marshall, A. G.; Qian, K. Kendrick mass defect spectrum: A compact visual analysis for ultrahigh-resolution broadband mass spectra. *Anal. Chem.* **2001**, *73*, 4676–4681.

(6) Panda, S. K.; Brockmann, K. J.; Benter, T.; Schrader, W. Atmospheric pressure laser ionization (APLI) coupled with Fourier transform ion cyclotron resonance mass spectrometry applied to petroleum samples analysis: Comparison with electrospray ionization and atmospheric pressure photoionization methods. *Rapid Commun. Mass Spectrom.* **2011**, *25*, 2317–2326.

(7) Lias, S. G.; Ausloos, P. Ionization energies of organic compounds by equilibrium measurements. *J. Am. Chem. Soc.* **1978**, *100*, 6027–6034.

(8) Ladavie`re, C.; Desmazes, P. L.; Delolme, F. First systematic MALDI/ESI mass spectrometry comparison to characterize polystyrene synthesized by different controlled radical polymerizations. *Macromolecules* **2009**, *42*, 70-84.

(9) Gross, J. H. Chemical Ionization, In *Mass spectrometry*, 2nd ed.; Springer-Verlag, Heidelberg, **2004**, pp. 341-344.

(10) Gu, M.; Turecek, F. Fingerprinting stereoisomers by survivor-ion mass spectrometry. *Org. Mass Spectrom.* **1994**, *29*, 85-89.

(11) Boesl, U.; Zimmermann, R.; Weickhardt, C.; Lenoir, D.; Schramm, D. W.; Kettrup, A.; Schlag, E. W. Resonance-enhanced multi-photon ionization: A species-selective ion source for analytical time-of-flight mass spectroscopy. *Chemosphere* **1994**, *29*, 1429–1440.

(12) Imasaka, T. Gas chromatography/multiphoton ionization/time-of-flight mass spectrometry using a femtosecond laser. *Anal. Bioanal. Chem.* **2013**, *405*, 6907–6912.

(13) Hanley, L.; Zimmermann, R. Light and molecular ions: The emergence of vacuum UV single-photon ionization in MS. *Anal. Chem.* **2009**, *81*, 4174–4182.

(14) Akhtar, Z. M.; Brion, C. E.; Hall, L. D. Mass spectral studies of stereoisomers: The photoionisation of some substituted cyclohexanols. *Org. Mass Spectrom.* **1973**, *7*, 647-666.

(15) Akhtar, Z. M. A photoionisation mass spectrometric study of stereoisomers. PhD thesis, University of British Columbia, Vancouver, Canada, 1972. https://open.library.ubc.ca/media/download/pdf/831/1.0060232/2 (accessed April 12, 2019).

(16) Matsumoto, J.; Lin, C. H.; Imasaka, T. Enhancement of the molecular ion peak from halogenated benzenes and phenols using femtosecond laser pulses in conjunction with supersonic beam/multiphoton ionization mass spectrometry. *Anal. Chem.* **1997**, *69*, 4524-4529.

(17) Li, A.; Uchimura, T.; Tsukatani, H.; Imasaka, T. Trace analysis of polycyclic aromatic hydrocarbons using gas chromatography–mass spectrometry based on nanosecond multiphoton ionization. *Anal. Sci.* **2010**, *26*, 841-846.

(18) Li, A.; Uchimura, T.; Watanabe-Ezoe, Y.; Imasaka, T. Analysis of dioxins by gas chromatography/resonance-enhanced multiphoton ionization/mass spectrometry using nanosecond and picosecond lasers. *Anal. Chem.* **2011**, *83*, 60-66.

(19) Yamaguchi, S.; Uchimura, T.; Imasaka, T. Gas chromatography/multiphoton ionization/mass spectrometry of polychlorinated dibenzofurans using nanosecond and femtosecond lasers. *Anal. Sci.* **2006**, *22*, 1483-1487.

(20) Kouno, H.; Imasaka, T. The efficiencies of resonant and nonresonant multiphoton ionization in the femtosecond region. *Analyst* **2016**, *141*, 5274–5280.

(21) Madunil, S. L.; Imasaka, T.; Imasaka, T. Resonant and non-resonant femtosecond ionization mass spectrometry of organochlorine pesticides. *Analyst* **2020**, *145*, 777-783.

(22) Hamachi, A.; Okuno, T.; Imasaka, T.; Kida, Y.; Imasaka, T. Resonant and nonresonant multiphoton ionization processes in the mass spectrometry of explosives. *Anal. Chem.* **2015**, *87*, 3027-3031.

(23) Zhu, X.: Lozovoy, V. V.; Shah, J. D.; Dantus, M. Photodissociation dynamics of acetophenone and its derivatives with intense nonresonant femtosecond pulses. *J. Phys. Chem. A* **2011**, *115*, 1305–1312.

(24) Schäfer, V.; Weitzel, K-M. Qualitative and quantitative distinction of *ortho-*, *meta-*, and *para-*fluorotoluene by means of chirped femtosecond laser ionization. *Anal. Chem.* **2020**, *92*, 5492−5499.

(25) Reusch, N.; Krein, V.; Wollscheid, N.; Weitzel, K-M. Distinction of structural isomers of benzenediamin and difluorobenzene by means of chirped femtosecond laser ionization mass spectrometry. *Z. Phys. Chem.* **2018**, *232*, 689-703.

(26) Kabo, G. J.; Frenkel, M. L. Thermodynamics of diastereomeric transformations of alcohols with different carbon-skeleton structures. *J. Chem. Thermodynamics* **1983**, *15*. 377-381.

(27) Bauernschmitt, R.; Ahlrichs, R. Treatment of electronic excitations within the adiabatic approximation of time dependent density functional theory. *Chem. Phys. Lett.* **1996**, 256, 454–464.

(28) Keldysh, L. V. Ionization in the field of a strong electromagnetic wave. *Sov. Phys. JETP* **1965**, *20*, 1307–1314.

(29) Ledingham, K. W. D.; Smith, D. J.; Singhal, R. P.; McCanny, T.; Graham, P.; Kilic, S.; Peng, W. X.; Langley, A. J.; Taday, P. F.; Kosmidis, C. Multiply charged ions from aromatic molecules following irradiation in intense laser fields. *J. Phys. Chem. A.* **1999**, *103*, 2952–2963.

(30) Pavia, D. L.; Lampman, G. M.; Kriz, G. S. Mass Spectrometry. In *Introduction to Spectroscopy*, 3nd ed.; Thomson learning, USA, 2001, pp. 390-465.

(31) Harrison, A. G.; Lin, M. S. Stereochemical applications of mass spectrometry. —Energy dependence of the fragmentation of stereoisomeric methylcyclohexanols. *Org. Mass Spectrom.* **1984**, *19*, 67-71.

Table 1. Ratio of signal intensities, $[M]^+/[M\text{-}H_2O]^+$, observed for 4-methylcyclohexanols.

	Techniques	$[M]^+/[M\text{-}H_2O]^+$
cis-4-methylcyclohexanol	Lyman-α source (121.6 nm, 10.2 eV)	1.21[14,15]
	He source (58.4 nm, 21.2 eV)	0.882[14,15]
	CECI ($C_6F_6^+$) (10.0 eV)	1.87[31]
	EI (70 eV)	0.611[31]
	UV 2PI (252 nm, 9.84 eV)	17.8 ± 1.04[a]
	NIR 10PI (1260 nm, 9.84 eV)	3.46 ± 0.19[a]
	EI (70 eV)	0.125[a]
trans-4-methylcyclohexanol	Lyman-α source (121.6 nm, 10.2 eV)	0.118[14,15]
	He source (58.4 nm, 21.2 eV)	0.0857[14,15]
	CECI ($C_6F_6^+$) (10.0 eV)	0.0877[31]
	EI (70 eV)	0.083[31]
	UV 2PI (257 nm, 9.63 eV)	1.00 ± 0.04[a]
	NIR 10PI (1260 nm, 9.84 eV)	0.22 ± 0.01[a]
	EI (70 eV)	ND[a]

[a] this study, ND; not detected

Figure Captions

Figure 1. Chemical structures of (A) *cis*- and (B) *trans*-4-methylcylohexanols.

Figure 2. Mass spectra measured by EI for (A) *cis*- and (B) *trans*-4-methylcyclohexanols. The *m/z* values of the fragment ions are indicated in the figure. M^+, molecular ion.

Figure 3. (A) Mechanisms of MPI using UV and NIR fs-lasers. (B) Signal intensities of the molecular and fragment ions. See the text for the explanations of processes (1) - (4).

Figure 4. Mass spectra of *cis*-4-methylcyclohexanol measured at different UV laser wavelengths; (A) 241 nm, (B) 245 nm, (C) 252 nm, (D) 257 nm, (E) 262 nm, (F) 267 nm.

Figure 5. Mass spectra of *trans*-4-methylcyclohexanol measured at different UV wavelengths; (A) 241 nm, (B) 245 nm, (C) 252 nm, (D) 257 nm, (E) 262 nm, (f) 267 nm.

Figure 6. Ratio of signal intensities measured for a molecular ion $[M]^+$ and a fragment ion observed at *m/z* = 96 $[M\text{-}H_2O]^+$ for (A) *cis*-4-methylcyclohexanol (B) *trans*-4-methylcyclohexanol at different UV wavelengths. The HWHM of the signal is shown in the figure. The data obtained by CECI ($C_6F_6^+$) and a VUVEI (Lyman-α) are also shown in the figure. The scales of single-photon (1P), two-photon (2P), and three-photon (3P) energies are indicated at the top of the figure.

Figure 7. Mass spectra of *cis*-4-methylcyclohexanol measured at different NIR wavelengths; (A) 1220 nm, (B) 1240 nm, (C) 1260 nm, (D) 1280 nm, (E) 1300 nm, (F) 1320 nm.

Figure 8. Mass spectra of *trans*-4-methylcyclohexanol measured at different NIR wavelengths; (A) 1220 nm, (B) 1240 nm, (C) 1260 nm, (D) 1280 nm, (E) 1300 nm, (F) 1320 nm.

Figure 9. Ratio of signal intensities measured for a molecular ion $[M]^+$ and a fragment ion observed at *m/z* = 96 $[M\text{-}H_2O]^+$ for (A) *cis*-4-methylcyclohexanol (B) *trans*-4-methylcyclohexanol at different NIR wavelengths. The data obtained by CECI ($C_6F_6^+$) and VUVEI (Lyman-α) are also shown in the figure. The scales of single-photon (1P), ten-photon (10P), and eleven-photon (11P) energies are indicated at the top of the figure. An arrow at 1318 nm indicates a position of the minimum expected to appear (see the text for details).

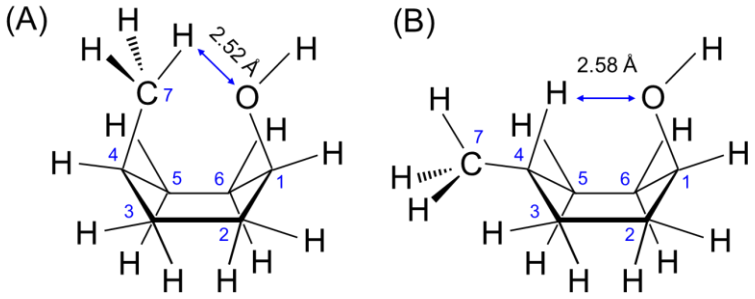

Fig. 1 S. Lakshitha Madunil et al.

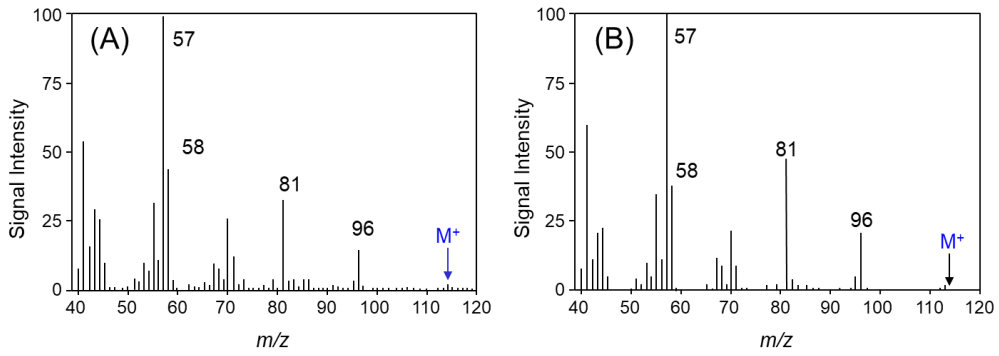

Fig. 2 S. Lakshitha Madunil et al.

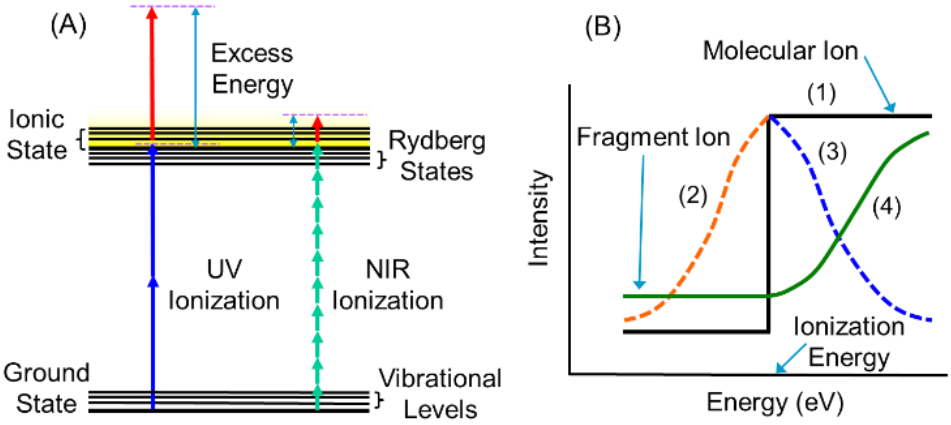

Fig. 3 S. Lakshitha Madunil et al.

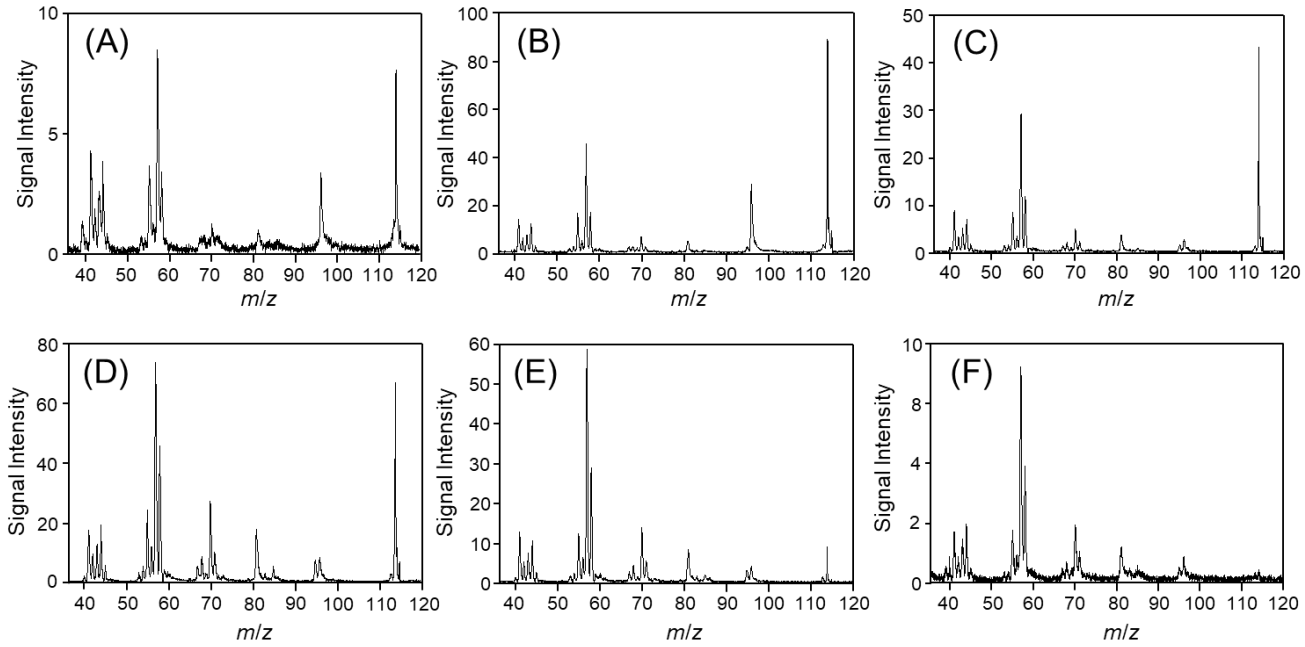

Fig. 4 S. Lakshitha Madunil et al.

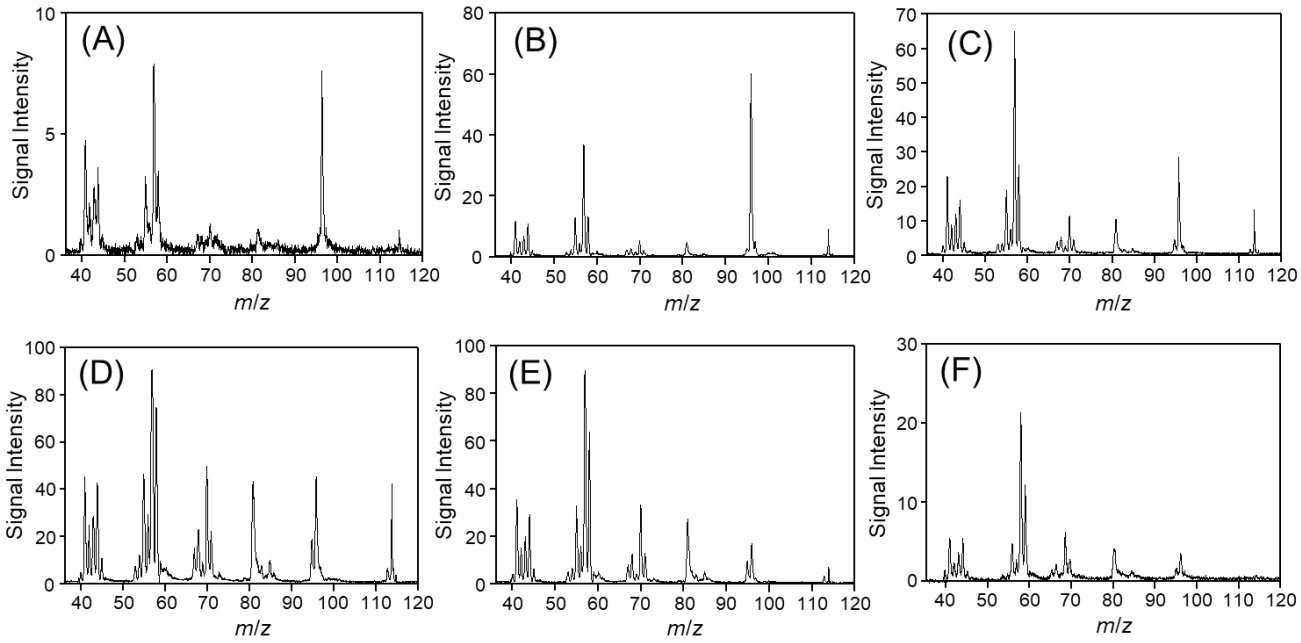

Fig. 5 S. Lakshitha Madunil et al.

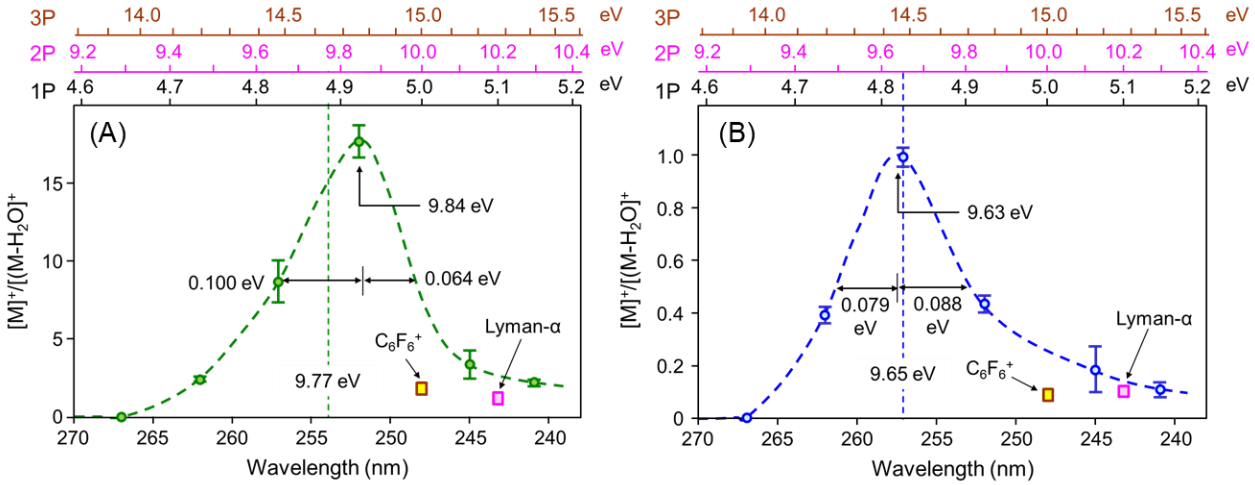

Fig. 6 S. Lakshitha Madunil et al.

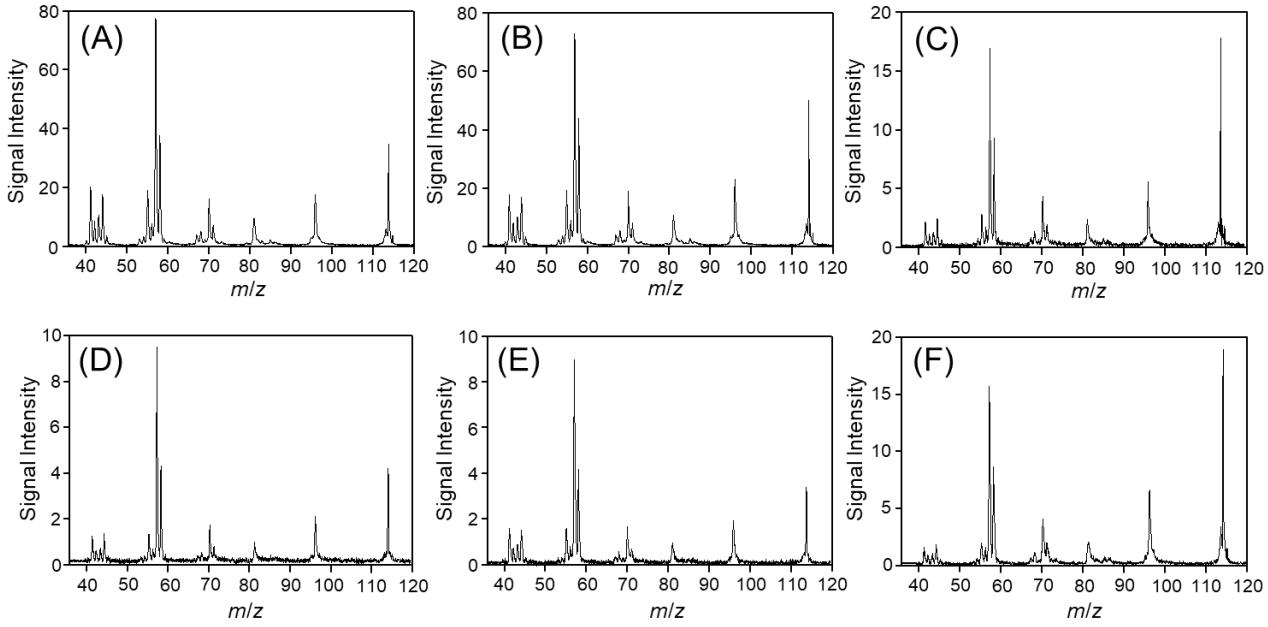

Fig. 7 S. Lakshitha Madunil et al.

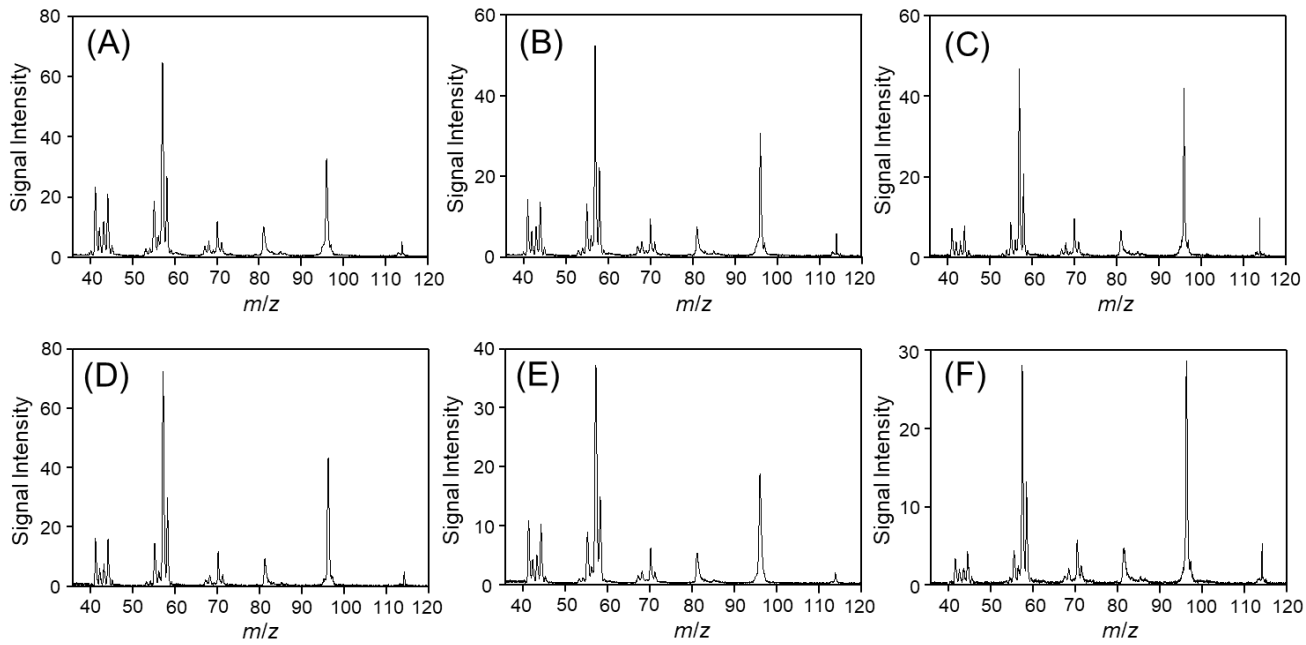

Fig. 8 S. Lakshitha Madunil et al.

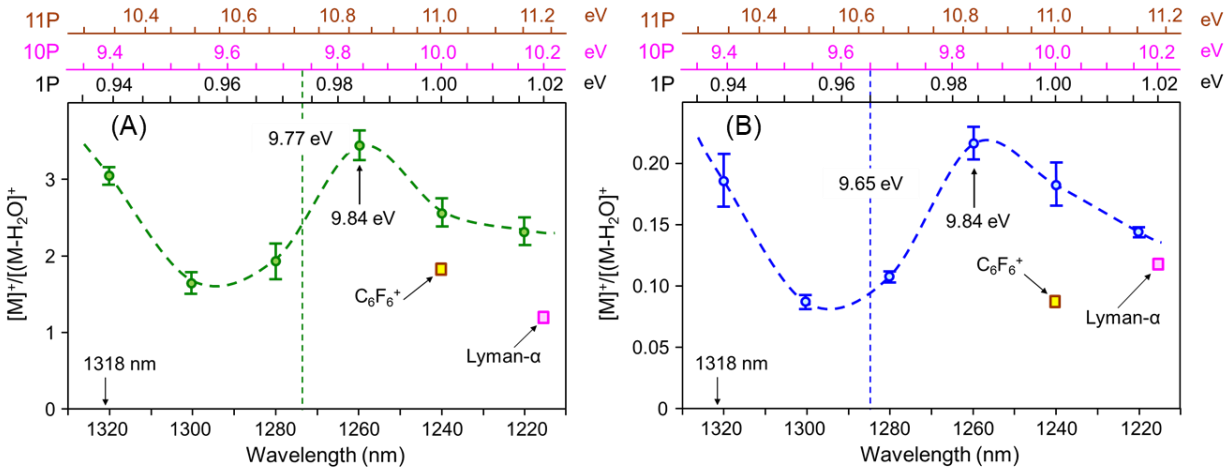

Fig. 9 S. Lakshitha Madunil et al.

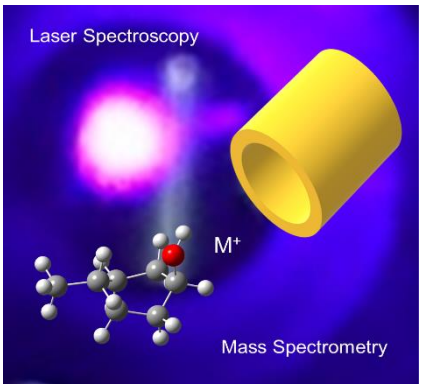

TOC